Veterinär-Anatomisches Institut
der Vetsuisse-Fakultät Universität Zürich

Direktor: Prof. Dr. Alois Boos

Arbeit unter wissenschaftlicher Betreuung von
PD Dr. Karl Rüdiger Klisch

Morphological Characterisation of Basally located Uninucleate Trophoblast Cells as Precursors of Bovine Binucleate Trophoblast Giant Cells

Inaugural-Dissertation

zur Erlangung der Doktorwürde der
Vetsuisse-Fakultät Universität Zürich

vorgelegt von

Jeannette Attiger

Tierärztin
aus Wetzikon (ZH)

genehmigt auf Antrag von

PD Dr. Karl Rüdiger Klisch, Hauptreferent

2018

Table of contents

Vetsuisse-Fakultät Universität Zürich (2018)

Jeannette Attiger

Veterinär-Anatomisches Institut, sekretariat@vetanat.uzh.ch

Morphological Characterisation of Basally located Uninucleate Trophoblast Cells as Precursors of Bovine Binucleate Trophoblast Giant Cells

Abstract

Binucleate trophoblast giant cells (TGCs) are one characteristic feature of the ruminant placenta. In cows, the frequency of TGCs remains constant over most time of pregnancy. As TGCs are depleted by their fusion with uterine epithelial cells, they need to be constantly formed while it is unclear whether they develop from stem cells (SCs) within the trophectoderm or whether they can arise from any uninucleate trophoblast cell (UTC). Within the latter theory, basally located uninucleate cells (BUCs) without contact to the feto-maternal interface would represent a transient cell between UTCs and TGCs. So far, no evidence for the existence of such transient cells or of SCs has been shown. The aim of the present study is to morphologically characterize early stages of TGC development. Placentomal tissue of 6 pregnant cows from different gestational stages (gestational days 51 - 214) was examined for BUCs, UTCs and TGCs either in serial sections (light and transmission electron microscopy (LM, TEM), n = 3), in single sections (TEM, n = 2) or by serial block face-scanning electron microscopy (SBF-SEM, n = 1). These investigations revealed the occurrence of BUCs as well as young basally located TGCs showing contact to the basement membrane (BM), but without apical contact to the feto-maternal interface. The study morphologically defines these two cell types as early stages of TGC development and shows that binucleation of TGCs can precede detachment from the BM.

Keywords: Placenta, Pregnancy, Cattle, Trophoblast giant cells, Stem cells

Vetsuisse-Fakultät Universität Zürich (2018)

Jeannette Attiger

Veterinär-Anatomisches Institut, sekretariat@vetanat.uzh.ch

Morphologische Charakterisierung von Basal gelegenen Uninukleären Trophoblastzellen als Vorläufer von bovinen binukleären Trophoblastriesenzellen

Zusammenfassung

Binukleäre Trophoblastriesenzellen (BTZs) sind ein Charakteristikum der Wiederkäuerplazenta. Der BTZ-Anteil im Trophektodern bleibt während langer Trächtigkeitsphasen konstant, wobei die BTZs durch Fusion mit uterinen Epithelzellen kontinuierlich zugrunde gehen. Dies setzt eine andauernde BTZ-Produktion voraus. Es wird diskutiert, ob die BTZs aus Stammzellen (SZs) im Trophektoderm oder aus normalen uninukleären Trophoblastzellen (NUZs) entstehen, wobei eine basal gelegene, uninukleäre Zelle (BUZ) ohne Kontakt zum maternalen Epithel eine Übergangzelle zwischen einer NUZ und einer BTZ darstellt. Beweise für die Existenz einer BUZ oder einer SZ wurden jedoch bisher nicht gezeigt. Das Ziel dieser Studie ist es, frühe Stadien der BTZ-Entwicklung morphologisch zu charakterisieren. Plazentomgewebe von 6 tragenden Kühen (Trächtigkeitstag 51 – 214) wurde licht- und transmissionselektronenmikroskopisch in Serienschnitten (n = 3), in Einzelschnitten (n = 2) oder im „serial block face-scanning electron microscope“ (n = 1) auf BUZs, NUZs und BTZs untersucht. Diese Untersuchungen bestätigten die Existenz von BUZs sowie von jungen, basal gelegenen BTZs mit Kontakt zur Basalmembran (BM) aber ohne Kontakt zum maternalen Epithel. Diese zwei Zelltypen werden anhand von morphologischen Kriterien als frühe Stadien der BTZ-Entwicklung interpretiert. Zudem wurde gezeigt, dass die Ablösung von der BM während der BTZ-Entwicklung nicht vor Erlangen eines binukleären Stadiums abgeschlossen sein muss.

Schlüsselwörter: Plazenta, Trächtigkeit, Rind, Trophoblastriesenzellen, Stammzellen

Morphological Characterisation of Basally located Uninucleate Trophoblast Cells as Precursors of Bovine Binucleate Trophoblast Giant Cells

Running title: Precursors of Binucleate Trophoblast Giant Cells

Jeannette Attiger, Alois Boos, Karl Klisch

Institute of Veterinary Anatomy, University of Zurich, Zurich, Switzerland

Keywords:

Placenta, Pregnancy, Cattle, Trophoblast giant cells, Stem cells

Abbreviations used in this paper:

BM	basement membrane
BNC	binucleate trophoblast cell
BUC	basally located uninucleate cell
DLB	double lamellar body
EMT	epithelial-mesenchymal transition
FS	fetal stroma
FV	fetal vessel
gd	gestational day
LM	light microscopy
ME	maternal epithelium
PAG	pregnancy-associated glycoprotein
PL	placental lactogen
PRP-I	pregnancy-related protein-I
rER	rough endoplasmic reticulum
SC	stem cell

SBF-SEM	serial block face-scanning electron microscopy
TE	trophoblast epithelium
TEM	transmission electron microscopy
TGC	trophoblast giant cell
TNV	total nuclear volume
UTC	uninucleate trophoblast cell
VLA-6	very late antigen-6

Abstract

Binucleate trophoblast giant cells (TGCs) are one characteristic feature of the ruminant placenta. In cows, the frequency of TGCs remains constant over most time of pregnancy. As TGCs are depleted by their fusion with uterine epithelial cells, they need to be constantly formed while it is still unclear whether they develop from stem cells (SCs) within the trophectoderm or whether they can arise from any uninucleate trophoblast cell (UTC). Within the latter, generally accepted theory, a basally located uninucleate cell (BUC) without contact to the feto-maternal interface would represent a transient cell between a UTC and a TGC. So far, no evidence for the existence of such transient cells or for the presence of SCs has been shown. The aim of the present study is to morphologically characterize early stages of TGC development. Placentomal tissue of 6 pregnant cows from different gestational stages (gestational days (gd) 51 - 214) was examined for BUCs, UTCs and TGCs either in serial sections (light and transmission electron microscopy (LM, TEM), n = 3), in single sections (TEM, n = 2) or by serial block face-scanning electron microscopy (SBF-SEM, n = 1). These investigations revealed the occurrence of BUCs, as well as young TGCs showing contact to the basement membrane (BM), but without apical contact to the feto-maternal interface. The study morphologically defines these two cell types as early stages of TGC development and shows that binucleation of TGCs can precede detachment from the BM.

Corresponding author:

Karl Klisch

Institute of Veterinary Anatomy, Vetsuisse Faculty, University of Zurich

Winterthurerstrasse 260, 8057 Zurich, Switzerland

E-Mail karl.klisch@uzh.ch

Phone +41 44 63 58785

Introduction

The trophoblast epithelium of the bovine placenta consists of uninucleate trophoblast cells (UTCs) and trophoblast giant cells (TGCs), also called binucleate trophoblast cells (BNCs) [Björkmann, 1969; Klisch et al., 1999a; Klisch et al., 1999b]. These two cell types are characteristic elements of the ruminant fetal placenta [Hoffman and Wooding, 1993; Wooding and Burton, 2008] with a morphology that is largely uniform within the different ruminant species [Wooding, 1992].

UTCs show a cuboidal to columnar shape [Wathes and Wooding, 1980], have contact to the trophectodermal basement membrane (BM) [Wimsatt, 1951] and their microvilli interdigitate with those of the uterine epithelial cells [Björkmann, 1969; Wathes and Wooding, 1980]. The cytoplasm shows polysomes, rough endoplasmic reticulum (rER) and a small Golgi apparatus. Their numerous mitochondria are located in the apical part of the cell while lipid droplets and vesicles of different size are situated near the BM [Björkmann, 1969; King et al., 1980].

TGCs are migrating cells, which develop in the basal part of the trophoblast epithelium [Wimsatt, 1951; Morgan and Wooding, 1983] and move apically to the feto-maternal contact zone to fuse with the uterine epithelium [Wathes and Wooding, 1980; Wooding and Wathes, 1980; Wooding, 1983]. Young, basally located TGCs [Wimsatt, 1951; Morgan and Wooding,

1983] do not have contact to the BM nor to the feto-maternal border [Hoffman and Wooding, 1993]. They possess a rounded shape and show a great amount of cytoplasmic ribosomes [Björkmann, 1968; Wooding, 1992]. Mature, apically migrating TGCs have an increased cell as well as nuclear volume [Morgan and Wooding, 1983; Wooding, 1992; Klisch et al., 1999b] and show numerous small mitochondria, plenty of rER and a large Golgi apparatus [Björkmann, 1968; Morgan and Wooding, 1983; Wooding, 1992]. They contain a remarkable amount of membrane-bound granules, which incorporate a variety of secretory proteins [Wooding and Beckers, 1987; Zoli et al., 1992; Klisch and Leiser, 2003]. Additionally, they possess a special organelle called double lamellar body (DLB), which has been claimed to be characteristic for TGCs while its function has not been described yet [Wooding and Burton, 2008].

The production of the cytoplasmic membrane-bound granules, which contain placental lactogen (PL) [Wooding and Beckers, 1987], prolactin-related protein-I (PRP-I) [Klisch and Leiser, 2003] and pregnancy-associated glycoprotein (PAG) [Zoli et al., 1992; Klisch and Leiser, 2003], displays an important function of TGCs. In cattle, the fusion of a TGC with a uterine epithelial cell forms a feto-maternal hybrid cell, which delivers the content of the cytoplasmic granules to the maternal tissue and circulation by basal exocytosis [Wathes and Wooding, 1980; Wooding, 1983; Wango et al., 1990]. As the feto-maternal hybrid cell degenerates after having transferred the content of the granules into the maternal tissue [Wooding and Wathes, 1980; Hoffman and Wooding, 1993], this protein delivery process implies a reduction of TGC number in the fetal tissue. However, their fraction within the trophectoderm is relatively consistent at about 20 % until the end of gestation [Wooding and Wathes, 1980]. Thus, a constant production of TGCs during pregnancy is required.

The origin of TGCs has been discussed by different authors, but is still not fully clarified. Wimsatt [1951] identified mature TGCs as “post-mitotic” cells due to the absence of cleavage-furrows in any TGC. He described the development of these cells by transforming

UTCs, which acquire a round shape, lose contact to the BM and become binucleate by acytokinetic mitosis [Wimsatt, 1951].

Greenstein et al. [1958] described an undifferentiated, polygonal to cuboidal cell type in the peri-implantational trophectoderm, which he construed to be a stem cell for both UTCs and TGCs [Greensteine et al., 1958].

The most recent and widely accepted theory about the origin of TGCs has been established by Wooding and his co-authors [Wooding, 1992; Wooding and Burton, 2008]. They suggest that any typical UTC can perform an asymmetric mitosis. One daughter cell of this mitosis is a basally located uninucleate cell (BUC), which subsequently develops into a TGC by losing contact to the BM and getting binuclear by an acytokinetic mitosis.

Despite these concepts have frequently been referred [Klisch et al., 1999a; Klisch et al., 1999b; Klisch and Leiser, 2003; Igwebuike, 2006; Haeger et al., 2016], to our knowledge, no evidentiary images for the existence of such a basally located uninucleate transient or stem cell in the mature bovine placenta have been published.

Thus, the aim of this study is to verify the existence of BUCs and to characterize the early stages of TGC development in cows morphologically. To settle these questions, amongst others, an automated serial sectioning technique (serial block face-scanning electron microscopy [SBF-SEM]), will be used.

Materials and Methods

TISSUE PREPARATION

Placental tissue was collected from 6 pregnant cows (gestational day (gd) 51, 109, 120, 140, 158 and 214) at a local slaughterhouse. Uteri were obtained approximately 30 min after death of the cow by bolt shoot and exsanguination. The gestational stage was estimated based on the measured fetal crown-rump length [Schnorr and Kressin, 2011].

Tissue from 5 of these cows (gd 51, 109, 120, 140, 214) was prepared for light microscopy (LM) and conventional transmission electron microscopy (TEM). One randomly chosen placentome was perfused with 20 ml 2.5 % glutaraldehyde in 0.1 M sodium/potassium (Na/K) phosphate buffer. For this perfusion, a fetal placental blood vessel close to the chosen placentome of the opened uterus was clipped with the tip of small scissors, a blunt 21G butterfly winged cannula (B. Braun Venofix 21G Butterfly Winged Cannula Needles, B. Braun Melsungen AG, Melsungen (Hessen), D) was introduced into the vessel and fixed with haemostats to the surrounding tissue to hold it in position. Then, perfusion was performed manually with soft pressure by a 20 ml syringe during 1-2 min without any pre-washes. A slice of 1 – 2 mm thickness and ranging from the top to the bottom of the placentome was cut out centrally of the placentome with a sharp razorblade and was trimmed to cubes of 1 - 2 mm side lengths with the same razorblade. These cubes were immersed in the same fixative as used for perfusion during 1h at 0 - 4°C. After fixation, the tissue was stored in cold 0.1 M Na/K phosphate buffer until it was postfixed with 1 % osmium tetroxide in 0.1 M Na/K phosphate buffer, dehydrated in a graded series of ethanol and embedded in epon. If necessary, the tissue cubes were trimmed to a size of 1 mm side lengths before postfixation.

For serial block face-scanning electron microscopy (SBF-SEM) one placentome of a pregnant cow (gd 158) was perfused with 20 ml 2.5 % glutaraldehyde and 2 % formaldehyde in 0.15 M cacodylate buffer (pH 7.4) containing 2 mM calcium chloride ($CaCl_2$). Perfusion was performed in the same way as perfusion of the tissue for LM and TEM. A slice of 1 – 2 mm thickness and ranging from the top to the bottom of the placentome was cut out centrally of the placentome with a sharp razorblade and was trimmed to cubes of 1 - 2 mm side lengths with the same razorblade. These cubes were immersed in the same fixative as used for perfusion during 3h at 0 - 4°C. Following fixation, the tissue was washed (4 x 3 min) in cold 0.15 M cacodylate buffer containing 2 mM $CaCl_2$ on a shaker and then stored in fresh buffer at 4°C until further processing. If necessary, the tissue cubes were trimmed to a size of 1 mm

side lengths before they were further treated following a protocol optimised for SBF-SEM [Deerinck et al., 2010]. Tissue embedding was mainly performed as described in this protocol except of two modifications: using an epon mixture with a harder consistence (3.63 g epoxy embedding medium (Fluka, Sigma-Aldrich Chemistry GmbH, Buchs, CH) + 2.63 g NMA (Nadic methyl anhydride, Fluka, Sigma-Aldrich Chemistry GmbH, Buchs, CH) + 1.25 g DDSA (Dodecenyl succinic anhydride, Fluka, Sigma-Aldrich Chemistry GmbH, Buchs, CH) + 0.14 g DMP-30 (2,4,6-Tris(dimethylaminomethyl)phenol, Fluka, Sigma-Aldrich Chemistry GmbH, Buchs, CH) for approximately 6 ml epon), which has been polymerized at 60°C during 2.5 days, and using Easy-Molds (EMS, Pennsylvania, USA).

SERIAL SECTION EXAMINATION

Light microscopy (LM)

Serial semithin sections (1 µm) were cut from tissue blocks of 3 animals (gd 51, 140 and 214) with an ultramicrotome (Ultracut E, Reichert, Vienna, AT), mounted on glass slides (Menzel-Gläser, Braunschweig, D) and stained with toluidine blue. Alternating, sections were either coverslipped in Pertex (Medite, Burgdorf, D) or left without a coverslip. Within the series of covered sections, several cells were followed and photographed with a light microscope. On the basis of the photographs, the cells were categorized in three groups: UTCs, which light microscopically were located on the BM and showed contact to the feto-maternal interface, TGCs, which exhibited two nuclei, or BUCs, which light microscopically did not show contact to the feto-maternal interface.

The nuclear volume of all examined cells was estimated according to the principle of Cavalieri [Mayhew, 1991] with the Stereoinvestigator software (MBF Bioscience, Williston, VT). In TGCs, the nuclear volumes of all nuclei in 1 cell were summed up as a total nuclear volume (TNV).

Transmission electron microscopy (TEM)

From each series of semithin sections, five non-coverslipped sections, with a distance of 6 µm (5 sections) between each other, were re-embedded in epon. Re-embedding was performed according to the protocol described by Suzuki et al. [2003], while instead of BEEM capsules [Suzuki et al., 2003] Easy-Molds (EMS, Pennsylvania, USA) were used. The re-embedded sections covered segments of the series where most of the light microscopically examined cells were located. After re-embedding, ultrathin sections (70 nm) were cut with an ultramicrotome (Ultracut E, Reichert, Vienna, AT), mounted on slot grids with formvar (EMS, Pennsylvania, USA) or polystyrene 2'000'000 g/mol membrane (0.5 g of polystyrene solved in 100 ml chloroform) and stained with uranyl acetate and lead citrate. The in LM examined cells were followed within the ultrathin sections with a transmission electron microscope (CM12, Philips, Eindhoven, NL) and photographs were taken with a CCD camera (Ultrascan 1000 or Orius 832, Gatan, Pleasanton CA, USA). By means of the photographs the cells were assessed regarding following criteria:

- contact to the BM
- contact to the feto-maternal interface
- presence of membrane-bound granules
- occurrence of particular organelles (DLB, mitochondria and free cytoplasmic ribosomes in all three cell types and Golgi apparatus and rER only in UTCs and BUCs)

In cases where none of the ultrathin sections of one semithin section were investigable due to rupture of the membrane or insufficient contrasting, an adjacent semithin section without coverslip was re-embedded, sectioned and examined.

Statistical Methods

Statistical analysis of the estimated nuclear volumes was done with SPSS 23 (IBM® SPSS® statistics, version 23.0, IBM Corp., USA).

SINGLE SECTION EXAMINATION

Transmission electron microscopy (TEM)

Ultrathin sections (70 nm) were cut from tissues of 2 animals (gd 109, 120) with an ultramicrotome (Ultracut E, Reichert, Vienna, AT), mounted on copper grids and stained with uranyl acetate and lead citrate. In 6 sections of each animal, TGCs were observed with a transmission electron microscope (CM12, Philips, Eindhoven, NL) and photographs were taken with a CCD camera (Ultrascan 1000 or Orius 832, Gatan, Pleasanton CA, USA). All TGCs, which were visible in a total cross section and showed two nuclei, were photographed. By means of the photographs, the cells were assessed regarding following criteria:

- contact to the BM
- contact to the feto-maternal interface
- presence of membrane-bound granules
- occurrence of DLB

SERIAL BLOCK FACE-SCANNING ELECTRON MICROSCOPY (SBF-SEM)

The prepared tissue of 1 animal (gd 158) was visualised in a serial block face-scanning electron microscope (FEI Quanta 250 FEG variable pressure SEM, Thermo Fischer Scientific) equipped with a Gatan 3View 2XP system and dedicated backscatter detector (Gatan, Inc., Pleasanton CA, USA). 2 areas, which contained chorionic villi, were imaged with a voxel size of 11 x 11 x 100 nm^3. Images had 5000 x 5000 pixels and stacks of 1000 images were produced.

SBF-SEM images were edited with ImageJ (ImageJ, version 2.0.0-rc-43/1.51d, open source image processing software) as followed: inversion, smoothing, contrast enhancement of 0.5 %

and conversion from 16-bit dm3-data file to 8-bit tiff-data file. Image stacks were screened for BUCs, of which 1 cell was reconstructed to a three-dimensional image. Therefore, the selected cell was manually segmented with the ImageJ plugin TrakEM2. Cell nucleus, cell body and the trophoblast epithelium were segmented separately in a stack of images and a three-dimensional model was created with the Imaris x64 9.0.0 (Bitplane AG) software.

Results

SERIAL SECTION EXAMINATION

Light microscopy (LM)

In series of semithin sections, 63 TGCs, 20 BUCs and 65 UTCs were followed (Fig. 1 a, b) and their TNVs were determined. The TNVs of TGCs showed a wide variation and ranged from 491 to 2777 μm^3. TNVs of BUCs and UTCs showed both a unimodal distribution and ranged from 298 to 607 μm^3 (BUCs) and from 161 to 679 μm^3 (UTCs) respectively. All measured TNVs are presented in histograms (Fig. 2 a-c). The TNV of those cells which were examined by LM and TEM are also given in tables (supplementary data: tables 1, 2 and 3).

Transmission electron microscopy (TEM)

Since the morphological characteristics within each cell type did not show distinctions between the different gestational stages, cells from several animals are not described separately. Some cells could not be unambiguously assigned to 1 cell type (TGC, BUC or UTC) based on TEM. These cells as well as cells which could be examined on ultrathin sections from only 1 semithin section, have been excluded from the ultrastructural evaluation. If the classification of the cell type differed between LM and TEM, the latter was regarded as valid.

Profiles of 32 TGCs were evaluated on ultrathin sections from 2 - 5 different semithin sections (supplementary data: table 1). In all three animals, TGCs with (n = 11) and without

(n = 17) contact to the BM were visible. All TGCs with contact to the BM did not show contact to the feto-maternal interface (Fig. 3 a, b) and only a few of them possessed membrane-bound granules (2 of 11) or DLB (1 of 11). The majority of TGCs with contact to the BM showed, subjectively evaluated, a higher amount of free cytoplasmic ribosomes compared to UTCs (9 of 11) and mitochondria were diffusely distributed within the cytoplasm (10 of 11). Approximately half of the TGCs with contact to the BM showed a thin layer of electron dense material associated with the inner surface of the cell membrane (5 of 11). This layer was either completely attached to the cell membrane, detached from the cell membrane in several places or completely detached from the cell membrane, but surrounding the main part of the cytoplasmic organelles. TNVs of all TGCs with contact to the BM ranged from 588 – 1326 μm^3.

The majority of TGCs without contact to the BM showed membrane-bound granules (12 of 17, Fig. 4 a, b), diffusely distributed mitochondria (16 of 17) and, subjectively evaluated, a higher amount of free cytoplasmic ribosomes compared to UTCs (13 of 17). A DLB was observed in 3 out of 17 TGCs without contact to the BM. Most of these cells showed a layer of electron dense material associated with the inner surface of the cell membrane as described above (16 of 17, Fig. 4 a, b). This layer of electron dense material was thicker compared to the one described in the TGCs with contact to the BM. In 2 TGCs without contact to the BM, contact to the feto-maternal interface was visible. The TNVs in all TGCs without contact to the BM varied between 508 and 2671 μm^3.

In 4 TGCs without contact to the feto-maternal interface, the contact to the BM could not definitely be ruled out nor confirmed while their cytoplasmic content showed similarities to TGCs with and without contact to the BM. Their TNVs varied between 2432 and 2777 μm^3.

Ultrastructural details of 9 BUCs were evaluated on ultrathin sections from 2 - 4 different semithin sections (supplementary data: table 2). All of the followed BUCs showed contact to the BM but no contact to the maternal epithelium (Fig. 5 a - d). A DLB was visible in 2 cells

(Fig. 1 a) and no cell showed cytoplasmic membrane-bound granules or a layer of electron dense material as found in the TGCs. The Golgi apparatus was not visible in any section of BUCs and rER as well as mitochondria were rarely found in all examined BUCs. In most sections, where mitochondria were visible, they seemed to be diffusely distributed (in 8 of 9 BUCs). In 1 BUC, the amount of free cytoplasmic ribosomes was subjectively evaluated as higher compared to UTCs and, overall, nuclear-cytoplasmic ratio, also subjectively evaluated, appeared rather high in BUCs (Fig. 1 a and 5 a - d).

The morphology of 26 UTCs was evaluated on sections from 2 - 4 different semithin sections (supplementary data: table 3). All examined UTCs had contact to the feto-maternal interface and did not show membrane bound granules or DLB. Contact to the BM was visible in 23 cells while it was not (n = 1) or unclear (n = 2) represented in three cells. The distribution of mitochondria, which occurred in moderate amounts, varied between apical (12 of 26) and diffuse (14 of 26). In the majority of UTCs, electron dense material was visible in the apical cell part within the region of the interdigitating microvilli, but no layer of electron dense material was seen associated to the basolateral cell membrane (24 of 26, data not shown in supplementary data: table 3). A small Golgi apparatus was visible in 9 UTCs while small amounts of rER was seen in all UTCs.

SINGLE SECTION EXAMINATION

Cross sections of 62 binucleate TGCs were examined with TEM in single sections of two animals (supplementary data: table 4). In the majority of these cells, no contact to the BM was visible (n = 55, Fig. 4 a, b). Most of the TGCs without contact to the BM possessed membrane-bound granules (50 of 55) and showed a layer of electron dense material associated to the inner surface of the cell membrane as described in TGCs of serial sections (41 of 55, Fig. 4 a, b). In 10 TGCs without contact to the BM, a DLB was visible and 4 of the TGCs without contact to the BM showed contact to the feto-maternal interface.

Narrow attachments to the BM were found in 4 TGCs. None of these 4 cells revealed contact to the feto-maternal interface, membrane-bound granules nor a DLB. The majority of TGCs with contact to the BM had a layer of electron dense material associated to the inner surface of the cell membrane as described in TGCs of serial sections (3 of 4). In 3 TGCs, the contact to the BM could not definitely be ruled out nor confirmed while none of them had contact to the feto-maternal interface nor a DLB. Two of these cells possessed membrane-bound granules and 1 cell showed a layer of electron dense material associated to the inner surface of the cell membrane as described in TGCs of serial sections.

SBF-SEM

Within the images of SBF-SEM, 3 BUCs could be followed. These cells were located in the basal part of the trophoblast epithelium without contact to the maternal epithelium and possessed one nucleus. The three-dimensional structure of one of these cells is presented in Fig. 6 a. Detailed ultrastructural morphology could not be examined due to an insufficient resolution (Fig. 6 b).

Discussion

In the currently generally accepted hypothesis about the origin of ruminant TGCs, a BUC would represent the direct progenitor for a TGC [Wooding, 1992; Wooding and Burton, 2008]. To the authors' knowledge, such a BUC has never been revealed so far. This is probably due to the difficulty of accessing three-dimensional information about individual cells from two-dimensional sections. In our study, we used 2 different methods to gain three-dimensional information. On one hand we performed manual serial sectioning in LM and TEM, what allowed us to evaluate the presence or absence of contact to the apical or basal epithelial surface, number of nuclei per cell as well as nuclear volume and ultrastructural

information about the cytoplasmic content. In this method, information between the examined sections, called z-plane, got lost, while we obtained detailed information in the xy-plane by high resolution. On the other hand we utilized a more modern technique, the SBF-SEM, which allowed to reduce the loss of information in the z-plane (section thickness = 100 nm) compared to serial sectioning in TEM (distance between 2 examined sections = 6 μm). Even though, as it was necessary to view bigger areas containing chorionic villi, resolution in xy-plane had to be reduced to restrict the running-time of the SBF-SEM on a period of 62 hours. For these reasons, SBF-SEM offered more complete information about the presence or absence of contact to the apical and basal epithelial surface and enabled a clear three dimensional presentation of trophoblast epithelial cells, while cytoplasmic information was reduced. For both methods, tissue was perfused with fixative by a fetal placental vessel as the main interest was posed on the fetal trophoblast epithelium. Nevertheless, it is nicely visible on the images that the fetal epithelium and in particular the feto-maternal interface is well preserved without perfusion by a maternal placental vessel.

Even if the number of animals used in this study is relatively low, we consider the collected information as representative to answer the question posed in this study. This appears to be justified, first by the very detailed information obtained by the 2 serial-sectioning methods used in this study and, second by the fact that there are no indications about major, gestational-stage depending morphological variations within each trophoblast cell type from gestational day 45 until term [Björkmann, 1969], even though protein expression has been shown to vary within gestation [Green et al., 2000; Touzard et al., 2013].

A lack of contact to the BM is generally considered to be a distinctive feature of ruminant TGCs [Hoffman and Wooding, 1993; Wooding and Burton, 2008]. In our study, we showed for the first time that some binucleate TGCs still have narrow contact to the BM. Due to their basal location within the trophoblast epithelium and their relatively small TNVs, compared to all examined TGCs, we interpret these cells as early developmental stages of TGCs [Klisch et

al., 1999b]. These results indicate that the process of losing basal contact does not have to be completed before the cells become binucleate. Findings of previous studies showed, that alpha-keratin is localized in basally located binucleate cells, but not in mature, apically migrated cells [Lee et al., 1990]. This coincides with our results, as cytokeratin constitutes an important intracellular anchorage of hemidesmosomes, which attach epithelial cells to the BM [Alberts, 2015]. Nakano et al. [2001] showed that most bovine TGCs in culture, which expressed uniform cytoplasmic staining of PL, did not show a staining of cytokeratin. Only a very small minority of the PL-positive TGCs showed a weak staining of cytokeratin. Despite the interpretation of Nakano et al. [2001] that PL-producing TGCs did not have any cytokeratin, it seems possible for us, that this small minority of TGCs with simultaneous staining of PL and cytokeratin could correspond to TGCs found in our study showing contact to the BM as well as membrane-bound granules. Even though, as soon as PL production starts, cytokeratin expression decreases. This indicates that TGC maturation and migration is associated with a reciprocal regulation of these proteins [Nakano et al., 2001]. Therefore, as cytokeratin also represents the intracellular part of desmosomes [Getsios et al., 2004; Coch and Leube, 2016], we interpret desmosome-possessing TGCs, which have been shown by Morgan and Wooding [1983], as young stages of TGCs.

We observed an intracellular layer of electron dense material underlying the cell membrane of some TGCs and in relation to the microvilli of UTCs. Based on the ultrastructural appearance and the fact that actin is a main component of the microvilli frame in other epithelial cells [Fath and Burgess, 1995; Coch and Leube, 2016], we interpret this electron dense material in both cell types as a part of the actin cytoskeleton. This interpretation is reinforced by immunogold [Lang et al., 2004] and immunohistochemical stainings [Nakano et al., 2005]. Actin [Lang et al., 2004] as well as α6 and β1 integrin subunits and laminin [Pfarrer et al., 2003] have been suggested to be involved in TGC migration. As α6β1 integrin, also called very late antigen-6 (VLA-6) [Hemler et al., 1988], can interact indirectly with actin

389 intracellularly [Alberts, 2015] and with laminin extracellularly [Sonnenberg et al., 1988;
390 Alberts, 2015], the simultaneous staining of laminin and α6 and β1 integrin subunits along the
391 cell membrane of TGCs lead to the interpretation that these proteins cooperate in TGC
392 migration [Pfarrer et al., 2003]. Laminin and α6β1-integrin dependent cell movement has also
393 been described in epithelial cancer cells [Tani et al., 1997]. Another protein, which might be
394 involved in TGC migration, is E-cadherin [Nakano et al., 2005]. Nakano et al. [2005]
395 interpreted their findings of redistribution of E-cadherin from the membrane-associated
396 location to the cytoplasm in TGCs to play a role for TGC migration apically of tight
397 junctions. Down-regulation of membrane-associated E-cadherin has been described as an
398 event during epithelial-mesenchymal transition (EMT) in other tissues [Morali et al., 2001;
399 Yang and Liu, 2001]. EMT plays an important role in different biological processes such as
400 fetal development, tumour metastasis, renal interstitial fibrosis [Yang and Liu, 2001; Thiery,
401 2002; Yang and Weinberg, 2008] as well as in the development of extravillous
402 cytotrophoblast of the human placenta [Vicovac and Aplin, 1996; Davies et al., 2016]. Based
403 on the above-mentioned findings of Nakano and co-authors [2005], EMT might also play a
404 role in the development of bovine TGCs.
405 The presence of a BUC could be confirmed in all evaluated animals. Based on morphological
406 characteristics, we assume that these BUCs are the precursors of TGCs. Since TGCs migrate
407 from the basal part of the trophectodermal epithelium towards the maternal tissue [Wathes
408 and Wooding, 1980; Wooding and Wathes, 1980; Wooding, 1983], it appears obvious that
409 their direct progenitor is located within the basal part of the epithelium. Further, BUCs tend to
410 have narrow contacts to the BM (Fig. 5b, c), assuming that these cells are in the process of
411 losing contact to the BM, as it would be necessary for the development of TGCs.
412 Additionally, a DLB, which has been described to be a characteristic structure of TGCs
413 [Wooding and Burton, 2008], was shown in 2 BUCs.

According to Wooding and his co-authors [Wooding, 1992; Wooding and Burton, 2008], these BUCs would represent a transient cell between UTCs and TGCs. UTCs are morphologically and functionally distinct from TGCs [Igwebuike, 2006]. Consequently, such a development would be a transdifferentiation process, in which one differentiated cell undergoes a dedifferentiation into another specialized cell type [Rawlins and Hogan, 2006]. Differentiated cells have been shown to possess the ability for transdifferentiation in several other organs [Gordon and Lane, 1984; Michalopoulos et al., 2005].

In epithelial tissues that need continuous cell supply, proliferating cells can be separated into 2 groups: cells which show slow cycling activity and cells which show fast cycling activity. The slowly cycling cells are interpreted to be the tissue specific stem cells, which have the capability for self-renewal and give rise to cells of the second, fast cycling group. These fast cycling cells, the so-called “transit-amplifying” cells, have a reduced ability of self-renewal and arrange primarily supply to the sufficient number of specialized cells by progressive step-by-step differentiation and maturation [Lajtha, 1979; Potten and Loeffler, 1990; Tsujimura et al., 2002]. Transferred to the bovine trophoblast epithelium, it could be hypothesized that the UTCs, which show proliferative activity [Schuler et al., 2000], represent this “transit-amplifying” cell population and ensure the TGC ordnance by transdifferentiating. Findings of heterogeneous immunohistochemical staining of UTCs [Nishita et al., 1990] may reflect the step-by-step differentiation of these “transit-amplifying” cells. It remains open whether a slow cycling progenitor cell exists for the “transit-amplifying” UTCs.

Alternatively, it could be hypothesized that the BUCs represent a distinct stem cell population for the TGCs. Their basal localization within the trophoblast epithelium is reminiscent of epithelial stem cells in other tissues [Marei and Abd El-Gawad, 2001; Kurzrock et al., 2008]. Furthermore, their ultrastructural appearance, which has been assessed subjectively, seems to represent a rather high nuclear-cytoplasmic ratio and spare rER and mitochondria. These properties bear resemblance to the basal progenitor cells of the respiratory tract [Marei and

Abd El-Gawad, 2001]. Since we did not detect a Golgi apparatus in any of the BUCs, it is likely that these cells have only a small sized Golgi apparatus with low productivity. These observations raise the question as to whether BUCs could represent a cell population that differentiates into TGCs without having their origin in UTCs (Fig. 7 b). As no sign for fast cycling cells between BUCs and TGCs have been observed, in this new theory, BUCs would differentiate directly into post mitotic TGCs without morphological different "transit-amplifying" cells. There remains the option that the BUC population itself can be divided in a slow cycling cell group and a "transit-amplifying" cell group. To verify this hypothesis, further investigations would be needed, for example the combination of staining with proliferation marker and three-dimensional imaging.

In conclusion, we show that there is a basally located uninucleate cell type within the bovine trophoblast epithelium. The presence of such a cell type as an intermediate state between UTCs and TGCs has previously been postulated, but has never been revealed [Wooding, 1992; Wooding and Burton, 2008]. Based on morphological findings, we suggest, in accordance with Wooding and his co-authors [Wooding, 1992; Wooding and Burton, 2008], that the BUCs are the progenitor cells of TGCs. To clarify the question whether the BUCs themselves develop from UTCs [Wooding, 1992; Wooding and Burton, 2008] or if they are a separate self-replicating cell population (Fig. 7 a, b) needs further investigations.

Acknowledgements

The authors thank Miriam Lucas-Droste, Scientific Center for Optical and Electron Microscopy, ETH Zurich, for her guidance and the production of SBF-SEM images and to Moritz Kirschmann, Center of Microscopy and Image Analysis, University of Zurich, for his support with the image processing and 3D-modelling. We are grateful to Elisabeth Hoegger

and Elisabeth Schraner, Institute of Veterinary Anatomy, University of Zurich, for their technical advices and support with the light and electron microscopical imaging and Lutz Slomianka, Institute of Anatomy, University of Zurich, for his guidance and support with stereology. We also thank Jeanne Peter, Vetcom, University of Zurich, for graphical illustrations.

Conflicts of interest

The authors declare no conflicts of interest.

References

Alberts, B. (2015) Molecular biology of the cell. New York, NY, Garland Science, Taylor and Francis Group.

Björkmann, N.H. (1968) Fine structure of cryptal and trophoblastic giant cells in the bovine placentome. J Ultrastruct Res *24*: 249-258.

Björkmann, N.H. (1969) Light and electron microscopic studies on cellular alterations in the normal bovine placentome. Anat Rec *163*: 17-30.

Coch, R.A., R.E. Leube (2016) Intermediate filaments and polarization in the intestinal epithelium. Cells *5(3)*.

Davies, J.E., J. Pollheimer, H.E.J. Yong, M.I. Kokkinos, B. Kalionis, M. Knofler, P. Murthi (2016) Epithelial-mesenchymal transition during extravillous trophoblast differentiation. Cell Adhes Migr *10(3)*: 310-321.

Deerinck, T.J., E.A. Bushong, A. Thor, M.H. Ellisman (2010) NCMIR Methods for 3D EM: A new protocol for preparation of biological specimens for serial block face scanning electron microscopy. Microscopy *6-8*. https://ncmir.ucsd.edu/sbem-protocol accessed 07.12.17

Fath, K.R., D.R. Burgess (1995) Microvillus assembly. Not actin alone. Curr Biol *5(6)*: 591-593.

Getsios, S., A.C. Huen, K.J. Green (2004) Working out the strength and flexibility of desmosomes. Nat Rev Mol Cell Biol *5(4)*: 271-281.

Gordon, R.E., B.P. Lane (1984) Ciliated cell differentiation in regenerating rat tracheal epithelium. Lung *162(4)*: 233-243.

Green, J.A., S.C. Xie, X. Quan, B.N. Bao, X.S. Gan, N. Mathialagan, J.F. Beckers, R.M. Roberts (2000) Pregnancy-associated bovine and ovine glycoproteins exhibit spatially and temporally distinct expression patterns during pregnancy. Biol Reprod *62(6)*: 1624-1631.

Greenstein, J.S., R.W. Murray, R.C. Foley (1958) Observation on the morphogenesis and histochemistry of the bovine preattachement placenta between 16 and 33 days of gestation. Anat Rec *132*: 321-341.

Haeger, J.D., N. Hambruch, C. Pfarrer (2016) The bovine placenta in vivo and in vitro. Theriogenology *86(1)*: 306-312.

506 Hemler, M.E., C. Crouse, Y. Takada, A. Sonnenberg (1988) Multiple very late antigen (VLA)
507 heterodimers on platelets. Evidence for distinct VLA-2, VLA-5 (fibronectin receptor), and
508 VLA-6 structures. J Biol Chem *263(16)*: 7660-7665.
509 Hoffman, L.H., F.B.P. Wooding (1993) Giant and binucleate trophoblast cells of mammals. J
510 Exp Zool *266*: 559-577.
511 Igwebuike, U.M. (2006) Trophoblast cells of ruminant placentas -- A minireview. Anim
512 Reprod Sci *93(3-4)*: 185-198.
513 King, G.J., B.A. Atkinson, H.A. Robertson (1980) Development of the bovine placentome
514 from days 20 to 29 of gestation. J Reprod Fertil *59*: 95-100.
515 Klisch, K., W. Hecht, C. Pfarrer, G. Schuler, B. Hoffmann, R. Leiser (1999a) DNA-content
516 and ploidy level of bovine placentomal throphoblast giant cells. Placenta *20*: 451-458.
517 Klisch, K., R. Leiser (2003) In bovine binucleate trophoblast giant cells, pregnancy-associated
518 glycoproteins and placental prolactin-related protein-1 are conjugated to asparagine-linked N-
519 acetylgalactosaminyl glycans. Histochem Cell Biol *119(3)*: 211-217.
520 Klisch, K., C. Pfarrer, G. Schuler, B. Hoffmann, R. Leiser (1999b) Tripolar acytokinetic
521 mitosis and formation of feto-maternal syncytia in the bovine placentome: different modes of
522 the generation of multinuclear cells. Anat Embryol (Berl) *200(2)*: 229-237.
523 Kurzrock, E.A., D.K. Lieu, L.A. Degraffenried, C.W. Chan, R.R. Isseroff (2008) Label-
524 retaining cells of the bladder: candidate urothelial stem cells. Am J Physiol Renal Physiol
525 *294(6)*: 1415-1421.
526 Lajtha, L.G. (1979) Stem cell concepts. Differentiation *14(1-3)*: 23-33.
527 Lang, C.Y., S. Hallack, R. Leiser, C. Pfarrer (2004) Cytoskeletal filaments and associated
528 proteins during restricted trophoblast invasion in bovine placentomes: light and transmission
529 electron microscopy and RT-PCR. Cell Tissue Res *315(3)*: 339-348.
530 Lee, C.S., M.M. Ralph, K.J. Gogolinewens, M.R. Brandon (1990) Monoclonal-Antibody
531 (Sbu-1 and Sbu-3) identification of cells dissociated from the sheep pacentomal trophoblast. J
532 Histochem Cytochem *38(5)*: 649-652.
533 Marei, H.E.S., M. Abd El-Gawad (2001) Differentiation of ciliated cells in the terminal
534 bronchioles of neonatal calves. Eur J Morphol *39(5)*: 269-276.
535 Mayhew, T.M. (1991) The new stereological methods for interpreting functional morphology
536 from slices of cells and organs. Exp Physiol *76(5)*: 639-665.
537 Michalopoulos, G.K., L. Barua, W.C. Bowen (2005) Transdifferentiation of rat hepatocytes
538 into biliary cells after bile duct ligation and toxic biliary injury. Hepatology *41(3)*: 535-544.
539 Morali, O.G., V. Delmas, R. Moore, C. Jeanney, J.P. Thiery, L. Larue (2001) IGF-II induces
540 rapid beta-catenin relocation to the nucleus during epithelium to mesenchyme transition.
541 Oncogene *20(36)*: 4942-4950.
542 Morgan, G., F.B.P. Wooding (1983) Cell migration in the ruminant placenta: A freeze-
543 fracture study. J Ultrastruct Res *83*: 148-160.
544 Nakano, H., A. Shimada, K. Imai, T. Takahashi, K. Hashizume (2005) The cytoplasmic
545 expression of E-cadherin and beta-catenin in bovine trophoblasts during binucleate cell
546 differentiation. Placenta *26(5)*: 393-401.
547 Nakano, H., T. Takahashi, K. Imai, K. Hashizume (2001) Expression of placental lactogen
548 and cytokeratin in bovine placental binucleate cells in culture. Cell Tissue Res *303(2)*: 263-
549 270.
550 Nishita, T., C. Kinoshita, M. Maegaki, M. Asari (1990) Immunohistochemical studies of the
551 carbonic anhydrase isozymes in the bovine placenta. Placenta *11*: 329-336.
552 Pfarrer, C., P. Hirsch, M. Guillomot, R. Leiser (2003) Interaction of integrin receptors with
553 extracellular matrix is involved in trophoblast giant cell migration in bovine placentomes.
554 Placenta *24(6)*: 588-597.
555 Potten, C.S., M. Loeffler (1990) Stem cells: attributes, cycles, spirals, pitfalls and
556 uncertainties. Lessons for and from the crypt. Development *110*: 1001-1020.

557 Rawlins, E.L., B.L. Hogan (2006) Epithelial stem cells of the lung: privileged few or
558 opportunities for many? Development *133(13)*: 2455-2465.
559 Schnorr, B., M. Kressin (2011) Embryologie der Haustiere. Stuttgart, Enke.
560 Schuler, G., C. Wirth, K. Klisch, K. Failing, B. Hoffmann (2000) Characterization of
561 proliferative activity in bovine placentomes between day 150 and parturition by quantitative
562 immunohistochemical detection of ki67-antigen. Reprod Dom Anim *35*: 157-162.
563 Sonnenberg, A., P.W. Modderman, F. Hogervorst (1988) Laminin receptor on platelets is the
564 integrin VLA-6. Nature *336(6198)*: 487-489.
565 Suzuki, R., T. Domon, M. Wakita, T. Akisaka (2003) The reaction of osteoclasts when
566 releasing osteocytes from osteocytic lacunae in the bone during bone modeling. Tissue Cell
567 *35(3)*: 189-197.
568 Tani, T., A. Lumme, A. Linnala, E. Kivilaakso, T. Kiviluoto, R.E. Burgeson, L. Kangas, I.
569 Leivo, I. Virtanen (1997) Pancreatic carcinomas deposit laminin-5, preferably adhere to
570 laminin-5, and migrate on the newly deposited basement membrane. Am J Pathol *151*: 1289-
571 1302.
572 Thiery, J.P. (2002) Epithelial-mesenchymal transitions in tumour progression. Nat Rev
573 Cancer *2(6)*: 442-454.
574 Touzard, E., P. Reinaud, O. Dubois, C. Guyader-Joly, P. Humblot, C. Ponsart, G. Charpigny
575 (2013) Specific expression patterns and cell distribution of ancient and modern PAG in
576 bovine placenta during pregnancy. Reproduction *146(4)*: 347-362.
577 Tsujimura, A., Y. Koikawa, S. Salm, T. Takao, S. Coetzee, D. Moscatelli, E. Shapiro, H.
578 Lepor, T.T. Sun, E.L. Wilson (2002) Proximal location of mouse prostate epithelial stem
579 cells: a model of prostatic homeostasis. J Cell Biol *157(7)*: 1257-1265.
580 Vicovac, L., J.D. Aplin (1996) Epithelial-mesenchymal transition during trophoblast
581 differentiation. Acta Anat *156(3)*: 202-216.
582 Wango, E.O., F.B.P. Wooding, R.B. Heap (1990) The role of trophoblastic binucleate cells in
583 implantation in the goat: a morphological study. J Anat *171*: 241-257.
584 Wathes, D.C., F.B.P. Wooding (1980) An electron-microscopic study of implantation in the
585 cow. Am J Anat *159(3)*: 285-306.
586 Wimsatt, W.A. (1951) Observations on the morphogenesis, cytochemistry, and significance
587 of the binucleate giant cells of the placenta of ruminants. Am J Anat *89(2)*: 233-281.
588 Wooding, F.B. (1992) Current topic: the synepitheliochorial placenta of ruminants: binucleate
589 cell fusions and hormone production. Placenta *13(2)*: 101-113.
590 Wooding, F.B.P. (1983) Frequency and localization of binucleate cells in the placentomes of
591 ruminants. Placenta *4*: 527-540.
592 Wooding, F.B.P., J.F. Beckers (1987) Trinucleate cells and the ultrastructural localisation of
593 bovine placental lactogen. Cell and tissue research *247*: 667-673.
594 Wooding, F.B.P., D.C. Wathes (1980) Binucleate cell migration in the bovine placentome. J
595 Reprod Fertil *59*: 425-430.
596 Wooding, P., G.J. Burton (2008) Comparative placentation structures, functions and
597 evolution. Berlin, Springer.
598 Yang, J., Y. Liu (2001) Dissection of key events in tubular epithelial to myofibroblast
599 transition and its implications in renal interstitial fibrosis. Am J Pathol *159(4)*: 1465-1475.
600 Yang, J., R.A. Weinberg (2008) Epithelial-mesenchymal transition: At the crossroads of
601 development and tumor metastasis. Dev Cell *14(6)*: 818-829.
602 Zoli, A.P., P. Demez, J.-F. Beckers, M. Reznik, A. Beckers (1992) Light and electron
603 microscopic immunolocalization of bovine pregnancy-associated glycoprotein in the bovine
604 placentome. Biol Reprod *46*: 623-629.
605

606

607 **Figures**

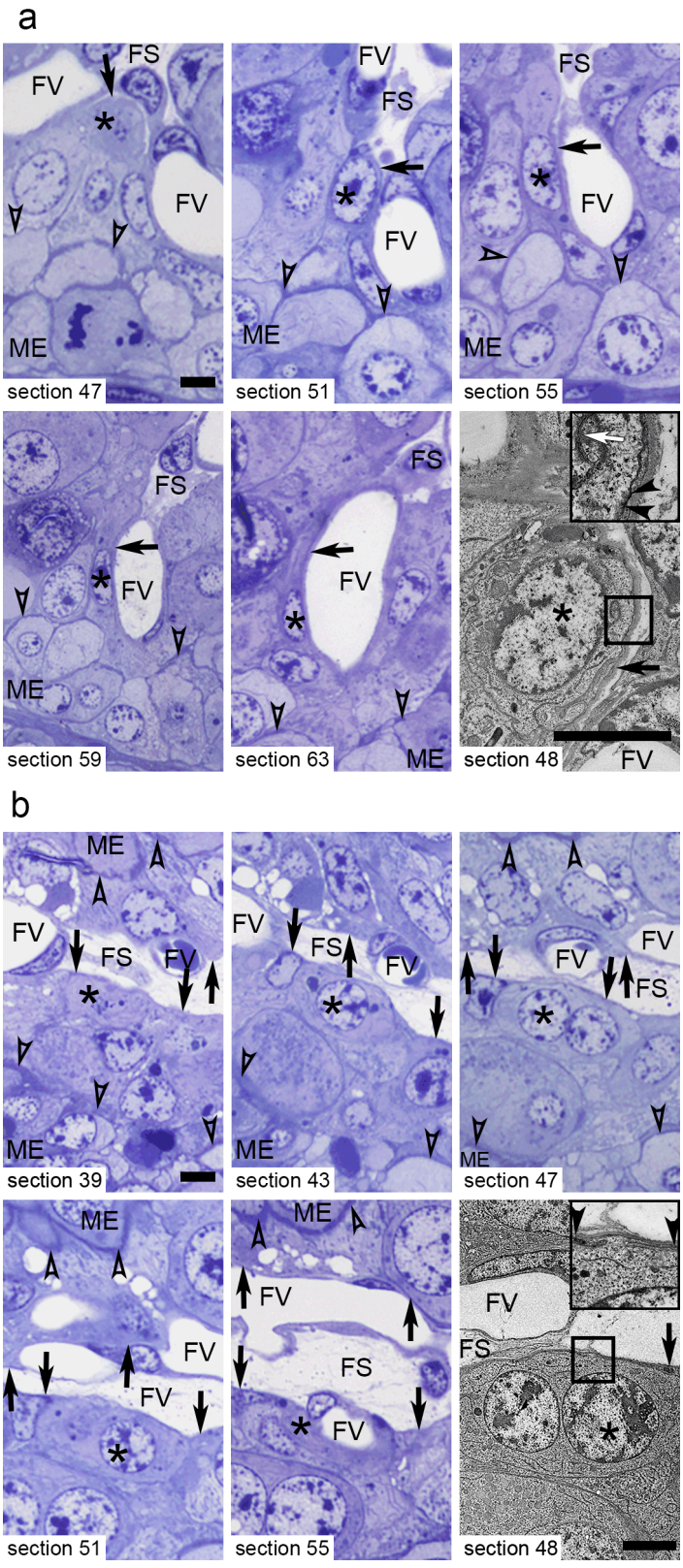

608

609 **Fig. 1 a, b.** Bovine trophoblast epithelium in serial sections of semithin sections in light
610 microscopy (LM) and an intermediate ultrathin section in transmission electron microscopy
611 (TEM) (FS: fetal stroma, FV: fetal vessel, ME: maternal epithelium, bars = 5 µm).

a Serial sections of a basally located uninucleate cell (BUC: asterisk) in LM (sections 47 – 63) with an intermediate TEM section (section 48). The inset in the TEM image of section 48 shows, that the BUC has contact to the basement membrane (BM: black arrows, contact is shown between black arrowheads in the inset at higher magnification) and a double lamellar body (DBL: white arrow). No contact to the feto-maternal interface (open arrowheads) was visible in the examined semithin or ultrathin sections and the nuclear-cytoplasmic ratio seems, subjectively evaluated, to be rather high (gd 140).

b Serial sections of a binucleate trophoblast giant cell (TGC: asterisk) in LM (sections 39 – 55) with an intermediate TEM section (section 48). This TGC shows contact to the BM (black arrows, contact is shown between black arrowheads in the inset at higher magnification). No contact to the feto-maternal interface (open arrowheads) was visible in the examined semithin or ultrathin sections (gd 140).

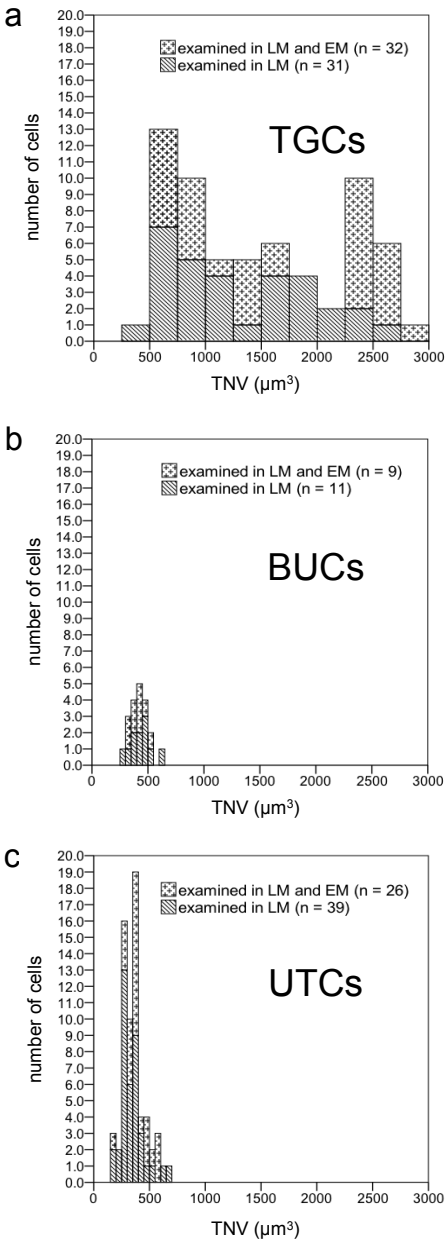

626

627 **Fig. 2 a-c.** Total nuclear volume (TNV in μm^3)

628 **a** Trophoblast giant cells (TGCs) show a wide variation of TNVs. Two peaks at about 600

629 and 2400 μm^3 are visible, which most likely correspond to TGCs with DNA contents of 2 x

630 2C and 2 x 8C [Klisch et al., 1999a; Klisch et al., 1999b].

631 **b** Basally located uninucleate cells (BUCs) and **c** uninucleate trophoblast cells (UTCs) show a
632 unimodal distribution of TNVs with lower values compared to the TGCs.
633
634

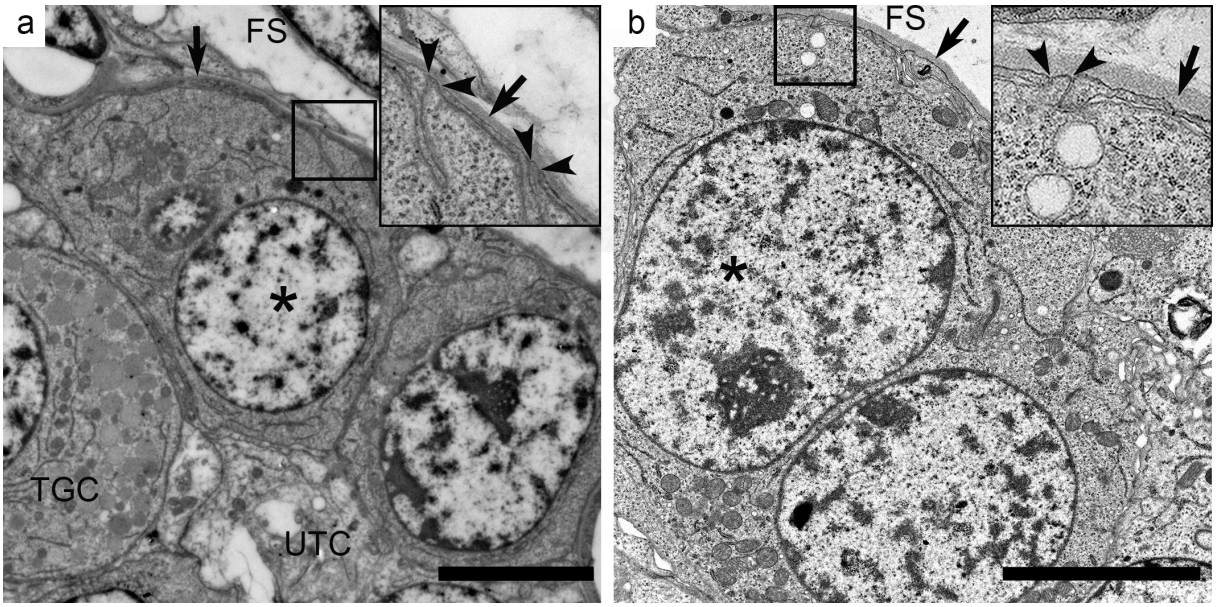

635
636 **Fig. 3 a, b**. Trophoblast giant cells (TGCs: asterisk) with contact to the basement membrane
637 (BM: black arrow, contact is shown between black arrowheads in the inset at higher
638 magnification). None of the TGCs with contact to the BM was in tangency to the feto-
639 maternal interface (FS: fetal stroma, bars = 5 μm).
640 **a** A binucleate TGC (asterisk) which reveals 2 narrow, tanged areas with contact to the BM
641 (between black arrowheads, gd 140).
642 **b** A binucleate TGC (asterisk) which reveals a narrow, tanged contact to the BM (between
643 black arrowheads, gd 109).
644

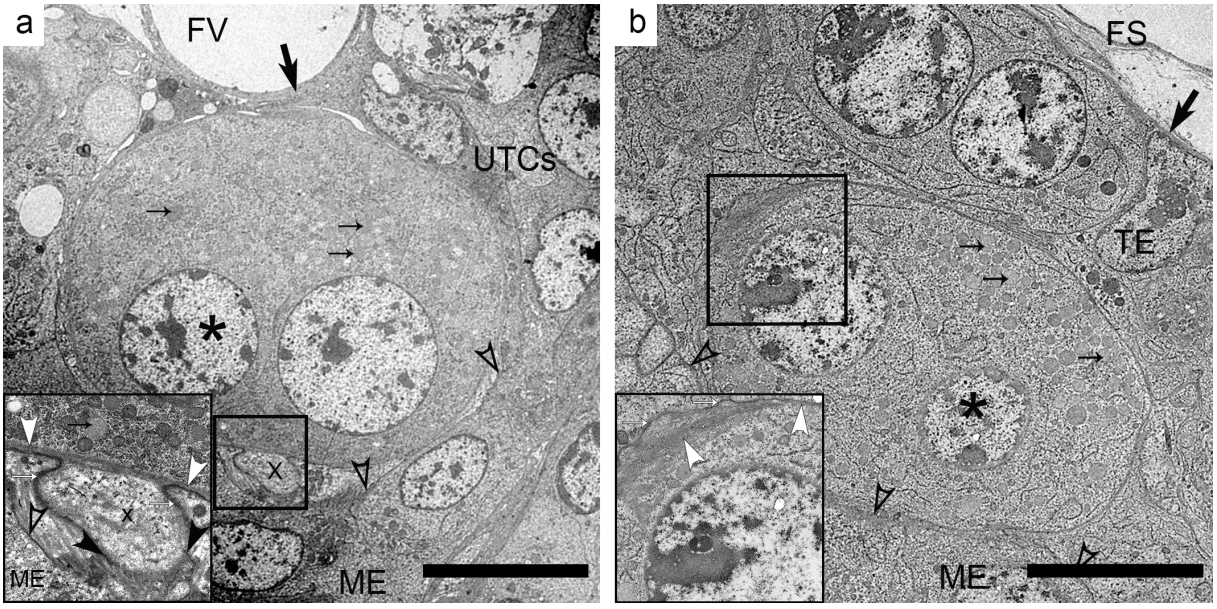

Fig. 4 a, b. Transmission electron microscopic sections of binucleate trophoblast giant cells (TGCs: asterisk) without contact to the basement membrane (BM: solid black arrow) and showing membrane bound granules (small black arrow) as well as intracellular electron dense material attached to the cellular membrane (white arrowheads). The areas in boxes are shown at higher magnification in the insets (FS: fetal stroma, FV: fetal vessel, TE: trophoblast epithelium, UTC: uninucleate trophoblast cell, open arrowheads: feto-maternal interface, bars = 10 µm).

a A binucleate TGC showing an apical protrusion (x), which is getting in contact with the maternal epithelium (ME). Along the inner surface of the cell membrane, a layer of electron dense material (white arrowheads) is visible, which excludes the apical protrusion (shown in the inset at higher magnification, gd 109).

b A binucleate TGC close to the maternal epithelium (ME). A layer of electron dense material (white arrowheads) is attached to the inner surface of the cell membrane (shown in the inset at higher magnification, gd 140).

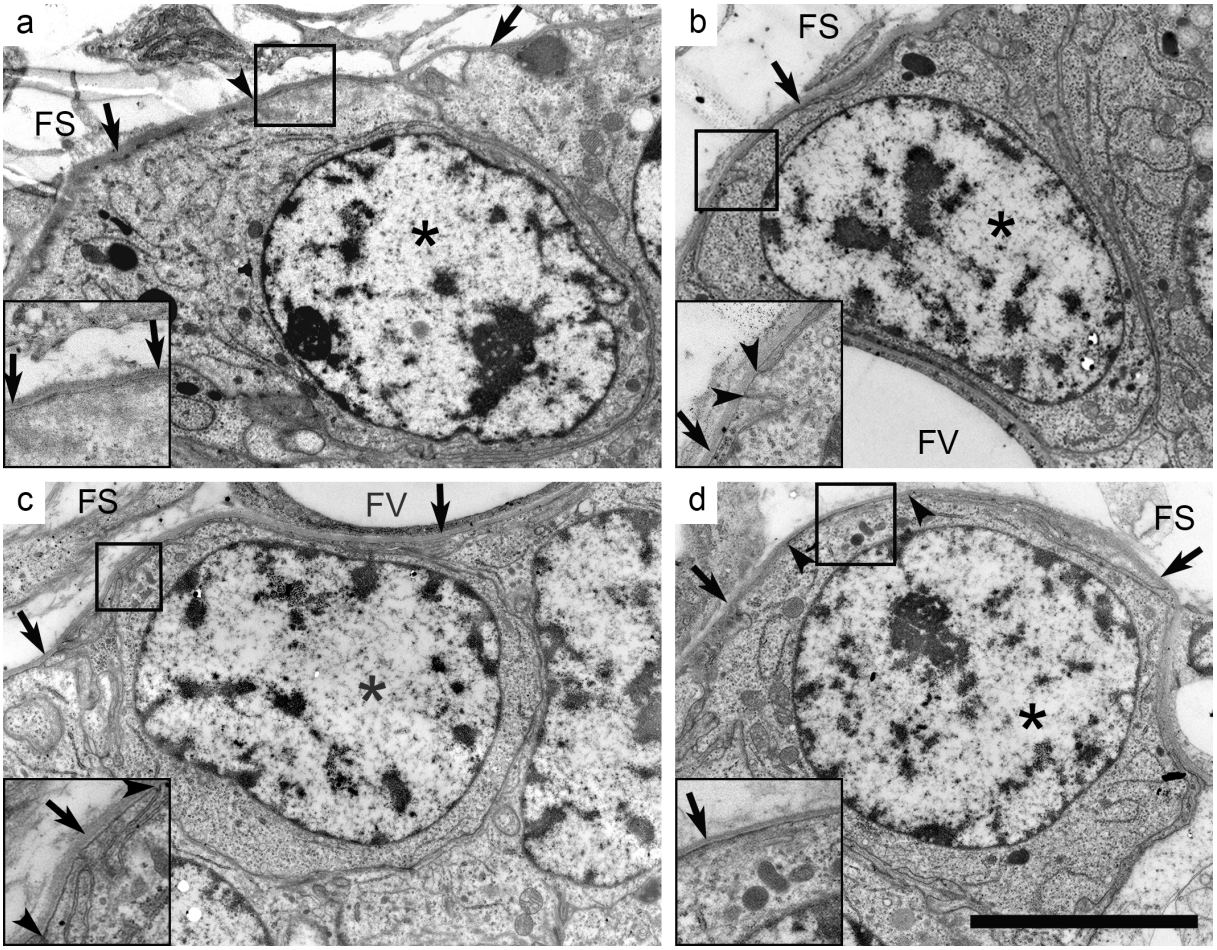

Fig. 5 a-d. Morphology of basally located uninucleate cells (BUCs: asterisk) of the bovine trophoblast epithelium. Contact to the basement membrane (BM: black arrows), which was visible in all examined BUCs, is shown at higher magnification in the insets. Nuclear-cytoplasmic ratio seemed, subjectively evaluated, to be rather high in BUCs. No examined BUC was in tangency with the feto-maternal interface (FS: fetal stroma, FV: fetal vessel, bar = 5 μm).

a, d A BUC with laminar contact to the BM (between black arrowheads, gd 214 and 140).

b, c A BUC with a petiolate contact to the BM (between black arrowheads, gd 140).

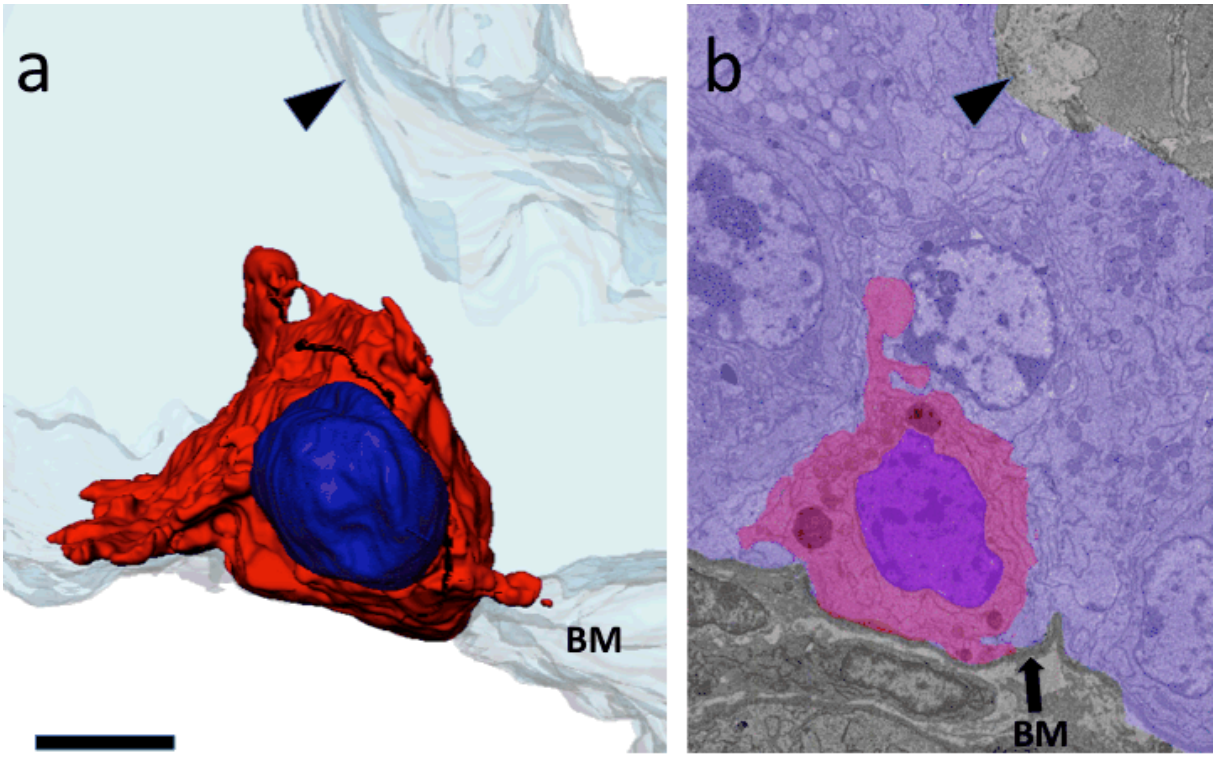

672

673 **Fig. 6 a.** Three-dimensional model of a basally located uninucleate cell (BUC), based on
674 serial block face-scanning electron microscopical images of the bovine trophoblast
675 epithelium. The cell has several basal processes and is attached to the basement membrane
676 (BM). No contact to the apical surface of the trophoblast epithelium (arrowhead) is present
677 (bar = 5 µm, gd 158).
678 **b** Serial block face-scanning electron microscopical image of the same cell as in image A of
679 this figure.

680

681

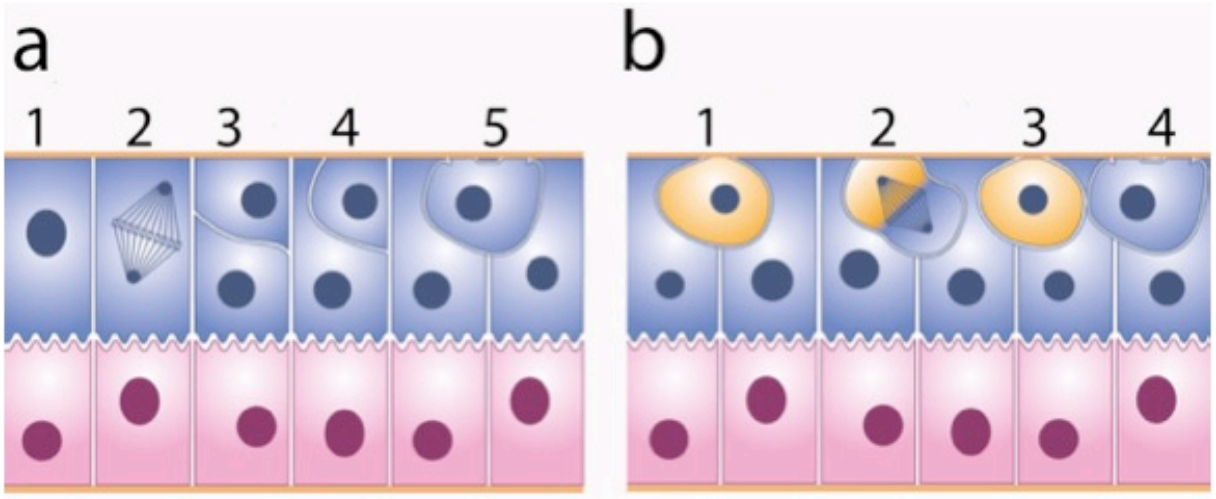

Fig. 7. Schematic drawings of 2 potential modes of the formation of basally located uninucleate cells (BUCs) in the bovine trophoblast epithelium. The fetal trophoblast epithelium is drawn on top, the maternal uterine epithelium is below.

a A typical UTC (1) undergoes an asymmetric mitosis (2) which leads to 2 different cells; 1 apically located cell and 1 basally located cell (BUC) (3). This latter cell gradually reduces the contact to the basement membrane (4 and 5).

b A basally located stem cell (yellow cell: 1) is present in the trophoblast epithelium. This cell performs a self-renewing asymmetric mitosis (2), which leads to 1 stem cell (yellow cell: 3) and 1 BUC (4).

Supplementary data

Table 1: TNV and ultrastructural characteristics of TGCs examined on serial sections, sorted after increasing TNV. (BM = basement membrane, FMI = feto-maternal interface, MBG = membrane-bound granules, FCR = free cytoplasmic ribosomes (compared to UTCs), LEDM = layer of electron dense material)

TNV (μm^3)	Contact to the BM	Contact to the FMI	Presence of MBG	Presence of DLB	Distribution of Mitochondria	Amount of FCR	Presence of a LEDM
508	no	no	no	no	diffuse	higher	yes
588	yes	no	no	no	mainly in basal part	higher	no
640	yes	no	no	no	diffuse	equal to UTCs	yes
659	yes	no	no	no	diffuse	higher	yes
678	yes	no	no	no	diffuse	higher	no
682	no	no	no	no	diffuse	higher	yes
756	yes	no	no	no	diffuse	higher	no
807	yes	no	no	no	diffuse	higher	yes
852	no	no	no	no	diffuse	higher	unclear but main part of organelles pushed to nuclei
936	yes	no	no	no	diffuse	higher	no
991	yes	no	no	yes	diffuse	higher	no
1131	yes	no	no	no	diffuse	higher	yes
1293	yes	no	yes	no	diffuse	equal to UTCs	no
1326	yes	no	yes	no	diffuse	higher	yes
1396	no	no	no	no	diffuse	higher	yes
1426	no	no	no	yes	diffuse	equal to UTCs	yes
1729	no	no	yes	no	mainly in side part	higher	yes
1742	no	no	yes	no	diffuse	higher	yes
2277	no	no	yes	no	diffuse	higher	yes
2314	no	no	yes	yes	diffuse	higher	yes
2338	no	yes	yes	no	diffuse	higher	yes
2359	no	no	yes	no	diffuse	higher	yes
2367	no	no	yes	no	diffuse	higher	yes
2432	unclear	no	yes	no	diffuse	equal to UTCs	unclear but main part of organelles pushed to nuclei
2441	no	yes	yes	no	diffuse	equal to UTCs	yes
2496	no	no	yes	no	diffuse	equal to UTCs	yes
2549	no	no	yes	no	diffuse	higher	yes
2561	no	no	yes	yes	diffuse	equal to	yes

						UTCs	
2626	unclear	no	yes	no	diffuse	higher	yes
2671	no	no	yes	no	diffuse	higher	yes
2694	unclear	no	yes	no	diffuse	unclear	yes
2777	unclear	no	yes	no	diffuse	higher	yes

Table 2: TNV and ultrastructural characteristics of BUCs examined on serial sections, sorted after increasing TNV. (BM = basement membrane, FMI = feto-maternal interface, MBG = membrane-bound granules, FCR = free cytoplasmic ribosomes (compared to UTCs), LEDM = layer of electron dense material)

TNV (μm^3)	Contact to the BM	Contact to the FMI	Presence of MBG	Presence of DLB	Distribution and amount of Mitochondria	Amount of FCR	Presence of a LEDM	Golgi visible	Amount of rER
318	yes	no	no	no	diffuse	equal to UTCs	no	no	rarely
324	yes	no	no	no	only a few present	equal to UTCs	no	no	rarely
352	yes	no	no	no	diffuse	equal to UTCs	no	no	rarely
386	yes	no	no	no	diffuse	higher	no	no	rarely
407	yes	no	no	no	diffuse	equal to UTCs	no	no	rarely
427	yes	no	no	yes	diffuse	equal to UTCs	no	no	rarely
438	yes	no	no	no	diffuse	equal to UTCs	no	no	rarely
456	yes	no	no	no	diffuse	equal to UTCs	no	no	rarely
537	yes	no	no	yes	diffuse	equal to UTCs	no	no	rarely

Table 3: TNV and ultrastructural characteristics of UTCs examined on serial sections, sorted after increasing TNV. (BM = basement membrane, FMI = feto-maternal interface, MBG = membrane-bound granules, LEDM = layer of electron dense material)

TNV (μm^3)	Contact to the BM	Contact to the FMI	Presence of MBG	Presence of DLB	Distribution of Mitochondria	Presence of a LEDM	Golgi visible	Amount of rER
191	yes	yes	no	no	mainly in apical part	no	no	rarely
268	yes	yes	no	no	mainly in apical part	no	yes	rarely
292	yes	yes	no	no	diffuse	no	no	rarely
296	yes	yes	no	no	diffuse	no	no	rarely
301	yes	yes	no	no	mainly in apical part	no	no	rarely
314	yes	yes	no	no	mainly in apical part	no	no	rarely
317	unclear	yes	no	no	diffuse	no	no	rarely
318	yes	yes	no	no	diffuse	no	no	rarely
354	unclear	yes	no	no	diffuse	no	yes	rarely
355	yes	yes	no	no	mainly in	no	no	rarely

					apical part			
359	yes	yes	no	no	mainly in apical part	no	yes	rarely
362	yes	yes	no	no	mainly in apical part	no	no	rarely
368	yes	yes	no	no	diffuse	no	no	rarely
370	yes	yes	no	no	mainly in apical part	no	yes	rarely
381	no	yes	no	no	diffuse	no	yes	rarely
386	yes	yes	no	no	mainly in apical part	no	no	rarely
387	yes	yes	no	no	diffuse	no	yes	rarely
388	yes	yes	no	no	mainly in apical part	no	no	rarely
420	yes	yes	no	no	diffuse	no	no	rarely
452	yes	yes	no	no	diffuse	no	no	rarely
464	yes	yes	no	no	mainly in apical part	no	yes	rarely
479	yes	yes	no	no	mainly in apical part	no	yes	rarely
512	yes	yes	no	no	diffuse	no	no	rarely
560	yes	yes	no	no	diffuse	no	no	rarely
565	yes	yes	no	no	diffuse	no	yes	rarely
599	yes	yes	no	no	diffuse	no	no	rarely

Table 4:Ultrastructural characteristics of TGCs examined on single sections. (BM = basement membrane, FMI = feto-maternal interface, MBG = membrane-bound granules, FCR = free cytoplasmic ribosomes (compared to UTCs), LEDM = layer of electron dense material)

Cell number	Contact to the BM	Contact to the FMI	Presence of MBG	Presence of DLB	Presence of a LEDM
1	no	no	yes	no	unclear but main part of organelles pushed to nuclei
2	no	no	yes	no	unclear but main part of organelles pushed to nuclei
3	no	no	yes	no	yes
4	no	no	yes	no	unclear but main part of organelles pushed to nuclei
5	no	no	yes	no	yes
6	no	no	yes	no	yes
7	no	no	yes	no	yes
8	no	no	no	no	no
9	no	no	yes	no	yes
10	no	no	yes	no	unclear but main part of organelles pushed to nuclei
11	no	no	yes	no	yes
12	no	no	yes	no	yes
13	no	yes	yes	no	yes
14	no	no	yes	no	unclear but main part

					of organelles pushed to nuclei
15	unclear	no	no	no	no
16	no	no	yes	no	yes
17	no	no	no	yes	no
18	unclear	no	yes	no	yes
19	no	no	yes	no	yes
20	no	no	yes	no	yes
21	no	unclear	yes	no	yes
22	unclear	no	yes	no	unclear but main part of organelles pushed to nuclei
23	no	no	yes	no	yes
24	no	no	yes	no	unclear but main part of organelles pushed to nuclei
25	no	no	yes	yes	no
26	no	unclear	yes	no	yes
27	no	no	yes	no	yes
28	no	no	yes	yes	yes
29	yes	no	no	no	no
30	no	no	yes	no	yes
31	no	no	yes	no	unclear but main part of organelles pushed to nuclei
32	no	no	yes	no	yes
33	no	no	yes	no	yes
34	no	no	yes	yes	yes
35	no	no	yes	unclear	yes
36	yes	no	no	no	yes
37	yes	no	unclear	unclear	yes
38	no	no	no	no	yes
39	no	no	yes	no	yes
40	no	no	yes	yes	yes
41	no	no	yes	no	yes
42	no	no	yes	no	yes
43	yes	no	no	no	yes
44	no	no	yes	yes	yes
45	no	no	yes	yes	yes
46	no	no	no	no	no
47	no	no	yes	no	yes
48	no	no	yes	yes	yes
49	no	no	yes	yes	yes
50	no	no	yes	no	yes
51	no	no	yes	no	yes
52	no	no	yes	no	yes
53	no	no	yes	yes	yes
54	no	yes	yes	no	yes
55	no	no	no	no	no
56	no	yes	yes	no	yes
57	no	no	yes	no	unclear but main part of organelles pushed to nuclei
58	no	no	yes	no	unclear but main part

					of organelles pushed to nuclei
59	no	yes	yes	no	yes
60	no	no	yes	no	yes
61	no	no	yes	no	yes
62	no	no	yes	no	yes

This is the peer-reviewed but unedited manuscript version of the following article: Cells Tissues Organs 2018;205(3):151-163 (DOI: 10.1159/000489257).
The final, published version is available at http://www.karger.com/?doi=10.1159/000489257

Curriculum Vitae

Vorname Name	Jeannette Attiger
Geburtsdatum	28. September 1989
Geburtsort	Wetzikon ZH
Nationalität	Schweiz
Heimatort bei Schweizern	Wetzikon ZH
08/2002 – 08/2008	Kantonsschule Zürcher Oberland, Wetzikon ZH
28.08.2008	Maturität (Kantonsschule Züricher Oberland, Wetzikon (CH))
09/2009 – 08/2014	Studium der Veterinärmedizin Vetsuisse-Fakultät, Universität Zürich (CH)
30.12.2014	Diplom med. vet. Vetsuisse-Fakultät, Universität Zürich (CH)
02/2015 – 05/2018	Anfertigung der Dissertation unter Leitung von PD Dr. med. vet. Karl Rüdiger Klisch Veterinär-Anatomisches Institut der Vetsuisse-Fakultät, Universität Zürich (CH) Direktor: Prof. Dr. Alois Boos
02/2015 – 04/2017	Assistenz in der Veterinär-Anatomischen Lehre Veterinär-Anatomisches Institut der Vetsuisse-Fakultät, Universität Zürich (CH)
05/2017 bis heute	Assistenztierärztin, Tierklinik Lindenhof, Bischofszell (CH)